Annals of Diagnostic Pathology 60 (2022) 152002

Contents lists available at ScienceDirect

Annals of Diagnostic Pathology

journal homepage: www.elsevier.com/locate/anndiagpath

Pleuropulmonary blastoma (PPB) and other *DICER1*-associated high-grade malignancies are morphologically, genetically and epigenetically related – A comparative study of 4 PPBs and 6 sarcomas

L.S. Hiemcke-Jiwa [a,b,*,1], S. van Belle [c,1], A. Eijkelenboom [c], J.H.M. Merks [a], M.M. van Noesel [a,d], S.E.J. Kaal [e], J.M.A. Pijnenborg [f], J. Bulten [c], B.B.J. Tops [a], C.P. van de Ven [a], J.M. van Gorp [g], R.R. de Krijger [a,b], E. Cheesman [h], A.M. Kelsey [h], L.A. Kester [a,1], U. Flucke [a,c,1]

[a] Princess Máxima Center for Pediatric Oncology, Utrecht, the Netherlands
[b] Department of Pathology, University Medical Center Utrecht, Utrecht, the Netherlands
[c] Department of Pathology, Radboud University Medical Center, Nijmegen, the Netherlands
[d] Division Imaging & Cancer, University Medical Center Utrecht, Utrecht, the Netherlands
[e] Department of Oncology, Radboud University Medical Center, Nijmegen, the Netherlands
[f] Department of Obstetrics and Gynecology, Radboud University Medical Center, Nijmegen, the Netherlands
[g] Department of Pathology, St Antonius Hospital, Nieuwegein, the Netherlands
[h] Department of Pathology, Central Manchester University Hospitals, Manchester, United Kingdom

ARTICLE INFO

Keywords:
DICER1
Pleuropulmonary blastoma
Rhabdomyosarcoma
Sarcoma
Methylation profiling
Whole transcriptome sequencing
Mutation analysis

ABSTRACT

DICER1-related tumors occur hereditary or sporadically, with high-grade malignancies sharing clinicopathological and (epi)genetic features. We compared 4 pleuropulmonary blastomas (PPBs) and 6 sarcomas by mutation analysis, whole transcriptome sequencing and methylation profiling.

9/10 patients were female. PPB patients were 0–4 years. 3/4 were alive; 2 without disease. One patient died of metastatic disease (median follow-up, 16 months). Sarcoma patients were 16–56 years. Locations included: uterine cervix/corpus (3/1), soft tissue back/shoulder (1) and paravertebral (1). 5/6 patients were alive; 2 developed metastases: intracranial (1) and lung and kidney (1) (median follow-up, 17 months). The deceased patient previously had a PPB and a Sertoli-Leydig cell tumor.

Histologically, tumors showed atypical primitive-looking cells with incomplete rhabdomyoblastic differentiation and cartilage (n = 5). Immunohistochemistry demonstrated desmin- (n = 9/10), myogenin- (n = 6/10) and keratin positivity (n = 1/1).

Eight cases harbored biallelic *DICER1* mutations with confirmed germline mutations in 4 cases. Two cases showed a monoallelic mutation.

By RNA expression- and methylation profiling, distinct clustering of our cases was seen demonstrating a close relationship on (epi)genetic level and similarities to embryonal rhabdomyosarcoma.

In conclusion, this study shows overlapping morphological, immunohistochemical and (epi)genetic features of PPBs and *DICER1*-associated high-grade sarcomas, arguing that these neoplasms form a spectrum with a broad clinicopathological range.

1. Introduction

DICER1-related tumors may occur sporadically or in an autosomal dominant fashion, the latter leading to the *DICER1*-related tumor susceptibility syndrome. The most well-known *DICER1*-associated malignancy is pleuropulmonary blastoma (PPB) with the most aggressive subtype designated as type 3 [1-3]. Based upon the presence of rhabdomyoblastic features, particularly in PPB type 3, this tumor was initially thought to represent a rhabdomyosarcoma (RMS) of the lung [4].

* Corresponding author at: Princess Maxima Center for Pediatric Oncology, Heidelberglaan 100, 3584 CX Utrecht, the Netherlands.
E-mail address: L.S.Jiwa-3@prinsesmaximacentrum.nl (L.S. Hiemcke-Jiwa).
[1] Authors contributed equally.

https://doi.org/10.1016/j.anndiagpath.2022.152002

Available online 25 June 2022

DICER1(syndrome)-related lesions are benign, such as cystic nephroma (CN), nodular goiter, nasal chondromesenchymal hamartoma and gastrointestinal hamartomatous polyps, as well as malignant, including genitourinary embryonal rhabdomyosarcoma (ERMS), Sertoli-Leydig cell tumor of the ovary, Müllerian adenosarcoma, Wilms tumor, anaplastic sarcoma of the kidney, pituitary blastoma, pineoblastoma, and well-differentiated thyroid carcinoma. Ocular medulloepithelioma, another *DICER*-associated tumor, may behave in a benign or malignant fashion [1,3,5-17]. Furthermore, development of a malignant tumor in a benign lesion has also been reported, e.g. anaplastic sarcoma of the kidney arising in cystic nephroma [10,18].

New entities have recently been added to this list, such as *DICER1*-associated central nervous system sarcoma [19], presacral malignant teratoid neoplasm [20], malignant teratoma of the thyroid [21], childhood- and adolescent-onset poorly differentiated thyroid carcinoma [22], ovarian sarcoma and PPB-like peritoneal sarcoma [1,23-25].

The morphology of the high-grade malignancies is similar with variable presence of primitive spindle and round cells with blastemal features and anaplasia. In addition, a rhabomyoblastic component and fetal-like or sarcomatous cartilage may be characteristically identified [1]. (Neuro)epithelial structures are described mainly in lesions called malignant teratoma or teratoid neoplasm, but have also been reported in other *DICER1*-associated malignancies [20,21,26].

On the epigenetic level, *DICER1*-related intracranial sarcomas show a distinct signature according to array-based genome-wide DNA methylation profiling corresponding to *DICER1* mutated uterine ERMSs [27,28].

These observations prompted us to investigate and compare the genetic features on the DNA and RNA level and the epigenetic/methylation profile of PPBs and *DICER1*-related sarcomas outside the lung and CNS.

2. Materials and methods

All cases were collected from the authors (referral) files. Follow-up of all cases was updated until April 2022.

2.1. Histology and immunohistochemistry

Four μm thick sections from formalin-fixed paraffin embedded (FFPE) blocks were mounted on pre-coated slides and dried for at least 10 min at 56 °C. Subsequently, they were deparaffinized by xylene and rehydrated by ethanol. Sections were stained with hematoxylin and eosin (H&E) or by immunohistochemistry, using an automated Ventana tissue stainer (BenchMark Ultra, Roche). For pretreatment, slides were cooked in EDTA for 24 min (desmin, myogenin, CKAE1/3 and CK8/18) or 36 min (MyoD1) and incubated for 32 min with an antibody for: desmin (Novocastra, clone DER11, 1:50), myogenin (Roche, M7G007, ready to use), MyoD1 (Cellmarque, EP212, 1:25), CKAE1/3 (Roche, MA5-13156, ready to use) or CK8/18 (Roche, 22.1&23.1, ready to use).

2.2. Targeted gene panel sequencing

Targeted NGS was performed using an in house developed smMIPs sequencing panel in accordance with Steeghs et al. [29]. This technique is able to confidently call low frequency mutations in FFPE material. Sequencing was done on a NextSeq 500 (Illumina, San Diego, CA) following the manufacturer's instructions (300 cycles Mid-Output or High-Output sequencing kit), resulting in 2 × 150 bp paired-end reads. Demultiplexed FASTQ files were uploaded and analyzed in Sequence pilot version 4.4.0 (JSI medical systems, Ettenheim, Germany). All variants were manually inspected before clinical reporting.

2.3. Whole exome sequencing

Total DNA was isolated using the AllPrep DNA/RNA/Protein Mini Kit (Qiagen) according to standard protocol on the QiaCube (Qiagen). DNA-seq libraries were generated with 150 ng DNA using the KAPA HyperPrep Kit in combination with the HyperExome capture kit (Roche) and sequenced on a NovaSeq 6000 system (2 × 150 bp) (Illumina). The DNA sequencing data of the tumor and the normal reference material (DNA extracted from blood) were processed as per the GATK 4.0 best practices workflow for variant calling, using a wdl and Cromwell-based workflow (https://gatk.broadinstitute.org/hc/en-us/sections/360007226651-Best-Practices-Workflows). This included performing quality control with Fastqc (version 0.11.5) to calculate the number of sequencing reads and the insert size Picard (version 2.20.1) for DNA metrics output and MarkDuplicates [30].

2.4. RNA sequencing

Total RNA was isolated using the AllPrep DNA/RNA/Protein Mini Kit (Qiagen) in keeping with standard protocol on the QiaCube (Qiagen). For cases 1–4, 6 and 7, fresh frozen tissue was used, while in case 9 and 10 only FFPE was available. RNA-seq libraries were generated with 300 ng RNA using the KAPA RNA HyperPrep Kit with RiboErase (Roche) and subsequently sequenced on a NovaSeq 6000 system (2 × 150 bp) (Illumina). The RNA sequencing data were processed as per GATK 4.0 best practices workflow for variant calling, using a wdl and Cromwell-based workflow (https://gatk.broadinstitute.org/hc/en-us/sections/360007226651-Best-Practices-Workflows). This included performing quality control with Fastqc (version 0.11.5) to calculate the number of sequencing reads and the insert size Picard (version 2.20.1) for RNA metrics output and MarkDuplicates [30]. The raw sequencing reads were aligned using Star (version 2.7.0f) to GRCh38 and gencode version 29 [31].

2.5. Gene expression analysis

Gene expression counts were determined using Subread Counts [32] with default parameters on the deduplicated bam files and subsequently normalized to counts per million. Principle Component Analysis (PCA) was performed on the z-scored expression of the 5000 most highly variable genes across all samples used for analysis. This includes the *DICER1* sarcoma and PPB cases, but also embryonal and alveolar rhabdomyosarcomas that were used as reference. A umap was then generated based on the components of the PCA, with the alpha parameter set to 0.25.

2.6. Genome-wide DNA methylation profiling

DNA was isolated by NorDiag Arrow using the DiaSorin DNA extraction kit (NL) or GeneRead DNA FFPE Kit (Qiagen) according to the respective manufacturer's instructions. DNA concentration was measured using the Qubit 2.0 fluorometer. Per sample, we used 500 ng (DK) or 200 ng (NL) of DNA. Bisulphite conversion was performed with EZ DNA Methylation™ Kit (Zymo Research, Irvine, CA, USA). All methylation data were generated using the Illumina® MethylationEPIC (850 k) BeadChip platform as previously described [33]. Classification of the samples was performed by the Heidelberg sarcoma classifier using the version that was available at the time of diagnosis, either v10.1 of v12.2 [34].

3. Results

3.1. Clinical data

Four PPBs and six sarcomas were included. Clinical characteristics are depicted in Table 1.

All tumors except one occurred in females. The age of the patients affected with a PPB type 3 were 0–4 years (mean, 2 years). Follow-up ranged from 16 to 27 months (median, 16 months) with all except one patient being alive at last follow-up; patients 1 and 2 were without

Table 1
Clinical features of the study cohort.

Case	Sex	Age	Location of primary tumor	Pathological diagnosis	Other *DICER1* tumors	Metastasis	Treatment	Follow-up
1	F	11m	Lung	PPB type 3	No	No	Adjuvant chemotherapy	Aw/oD (16 m)
2	F	2y	Lung	PPB type 3	No	No	Neo-adjuvant + adjuvant chemotherapy	Aw/oD (16 m)
3	F	3y	Lung	PPB type 3	No	No	Neo-adjuvant + adjuvant chemotherapy	Aw/oD (in treatment)
4	M	4y	Lung	PPB type 3	No	Cerebral metastatic relapse (1y after diagnosis)	Adjuvant chemotherapy	DoD (27 m after diagnosis)
5	F	25y	Uterine cervix	ERMS	No	Cerebral metastatic relapse (4y after diagnosis)	Adjuvant chemo-radiotherapy	Aw/oD (17 m)
6	F	18y	Uterine cervix	ERMS	Unknown	Unknown	Unknown	Unknown
7	F	30y	Uterine cervix	ERMS	Unknown	Unknown	Unknown	Unknown
8	F	56y	Uterine corpus/ endometrium	Adenosarcoma	No	No	Uterus extirpation	Aw/oD (3.5y)
9	F	55y	Soft tissue left scapula	Sarcoma "NOS"	No	Lung and left kidney (22 m after diagnosis)	Adjuvant radiotherapy; palliative radio-chemotherapy	AwD (17 m)
10	F	16y	Paravertebral TH5	Sarcoma "NOS"	PPB[a] (13y ago); SLCT (1.5y ago)	No	Palliative radio-chemotherapy	DOD (7 months after diagnosis)

Abbreviations: F, female; M, male; m, months; y, years; Aw/oD, alive without disease; AwD, alive with disease; ERMS, embryonal rhabdomyosarcoma; DoD, dead of disease; SLCT, Sertoli-Leydig cell tumor.
[a] Type of PPB undetermined as resection was performed after treatment.

evidence of disease and patient 3 was alive with disease; patient 4 died after development of an intracranial metastasis 2 years after diagnosis.

Sarcoma patients had an age ranged from 16 to 56 years (mean, 33 years). Tumors occurred in the uterine cervix (n = 3), uterine corpus/ endometrium (n = 1), soft tissue of the scapula region (n = 1), and in the paravertebral soft tissue at the fifth thoracic vertebra (n = 1). Follow-up ranged from 17 months to 3.5 years (median, 17 months). All but one patient was alive at last follow-up. Two developed metastases: patient 5 an intracranial metastasis 4 years after diagnosis and patient 9 multiple lesions in both lungs as well as a metastasis in the left kidney 22 months after diagnosis. Patient 8 had no evidence of disease (last follow-up: 3.5 years), while in case 10 the patient died due to disease after 7 months, with a history of a PPB (13 years ago, at age 3 years) and a Sertoli-Leydig cell tumor of the ovary (SLCT, FIGO stage 1A; 1.5 years ago, at age 15 years).

3.2. Histopathology and immunohistochemistry

Of the PPBs, cases 1–3 showed a mixture of loosely arranged primitive looking cells including atypical spindle cells, rhabdomyoblasts, anaplastic cells, and blastemal elements (Fig. 1a). The nuclei were slightly polymorphic and heterochromatic. Mitotic and apoptotic figures were variably present. In addition, case 1 had fibrosarcoma-like areas with fascicles of monomorphic plump spindle cells. Case 4 primarily consisted of spindle cells with elongated and tapered nuclei and eosinophilic cytoplasm in keeping with rhabdomyoblastic differentiation. In two of the 4 cases (cases 2 and 3) foci of immature cartilage were observed. The vasculature was inconspicuous. By immunohistochemistry all PPBs expressed desmin in varying proportions, while myogenin and MyoD1 were only sparsely positive in case 2 and 3 (Fig. 1b). In contrast, the cerebral metastasis of case 4 stained for desmin and myogenin; MyoD1 was not performed.

Concerning the adolescent/adult sarcomas, cases 5–7 (uterine cervix) were polypoid, focally ulcerated and infiltrating, depicting a variable and especially subepithelial increased cellularity (cambium layer) (Fig. 2a). They consisted of vague bundles of slightly pleomorphic round to spindle cells and few obvious rhabdomyoblasts (Fig. 2b). The chromatin was heterogeneous with some hyperchromatic nuclei. There were some mitoses and apoptotic bodies. Also, an inflammatory reaction was seen. In case 7 multiple foci of primitive cartilage were additionally present. Immunohistochemically, there was partial expression of desmin and myogenin. The intracranial metastasis of case 5 showed increased cellularity with slightly pleomorphic tumor cells arranged in bundles, with mainly oval to elongated nuclei without obvious rhabdomyoblastic differentiation including absence of desmin, and only very focal and weak expression of myogenin.

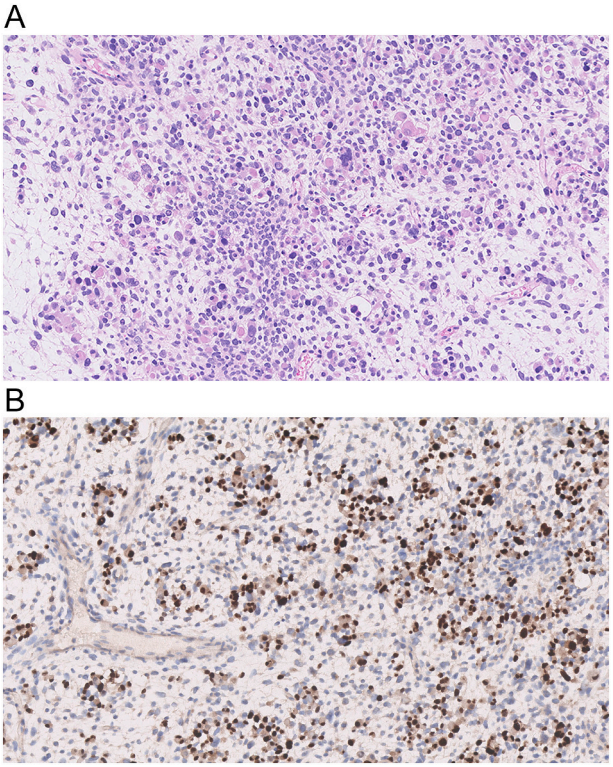

Fig. 1. a. Case 2 (PPB) demonstrates a mixture of loosely arranged primitive looking cells including atypical spindle cells, rhabdomyoblasts and anaplastic cells. Magnification 20×.
b. Case 2 (PPB) shows scattered nuclei with myogenin expression. Magnification 20×.

The tumor of case 8 (uterine corpus with extension into the cervix) was polypoid and infiltrated the myometrium. It consisted of atypical

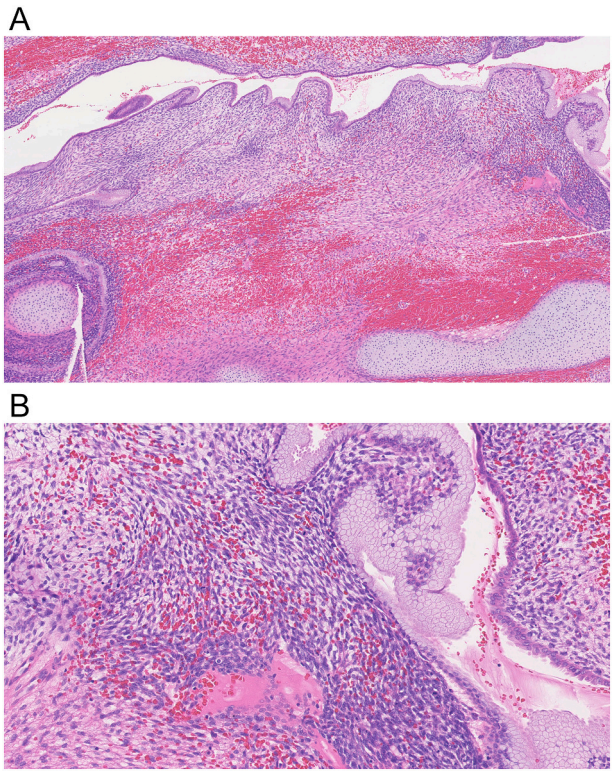

Fig. 2. a. In Case 7 (sarcoma of the uterine cervix) a subepithelial cell condensation (cambium layer) and primitive cartilage were obvious. Magnification 6×.
b. Vague bundles of slightly pleomorphic spindle cells and few obvious rhabdomyoblasts are present in Case 7. Magnification 20×.

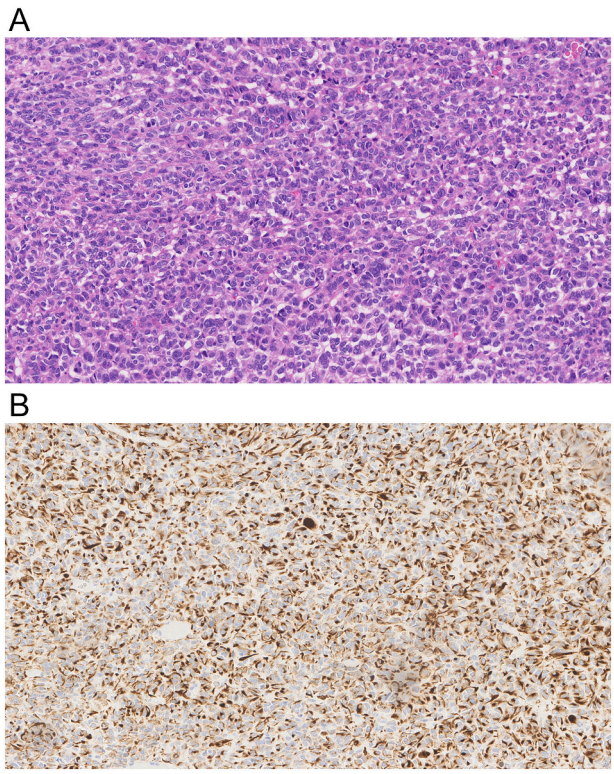

Fig. 3. a. Case 9 (soft tissue sarcoma (shoulder)) is defined by a diffuse sheet-like proliferation of epithelioid cells with slightly pleomorphic nuclei. Magnification 20×.
b. Diffuse expression of CK8/18 was only observed in Case 9. Magnification 20×.

primitive spindle cells with alternating cellularity with prominent periglandular condensation. There were few rhabdomyoblasts, some anaplastic cells and some multinucleated cells. Mitoses and apoptotic bodies were scattered throughout. Focally, nodules of primitive cartilage were apparent. The overlying and entrapped glandular epithelium had no atypia. By immunohistochemistry, desmin was focally expressed and myogenin was partially positive.

Case 9 was an infiltrating multinodular soft tissue lesion displaying a diffuse sheet-like proliferation of epithelioid cells with enlarged, slightly pleomorphic round to oval nuclei with open chromatin without prominent nucleoli (Fig. 3a). The cytoplasm was mainly scant and clear to eosinophilic. Some multinucleated cells were seen. Mitoses, including atypical forms, and apoptotic debris were frequently present. Dilated blood vessels and hemorrhage were encountered. Immunohistochemically, the cells showed dot-like expression of desmin, without the presence of myogenin. In addition, the tumor cells were diffusely positive for pankeratin AE1/3 and keratin 8/18 (Fig. 3b). The biopsy of the metastasis in the kidney had a similar appearance with additional foci of necrosis.

Case 10, a soft tissue lesion, showed an infiltrative proliferation of primitive spindle cells arranged in sheets, with minimal amounts of clear to pale eosinophilic cytoplasm but without obvious rhabdomyoblastic differentiation. The nuclei were oval and tapered with condensed chromatin. There were multiple mitoses and also apoptotic bodies. Focally necrosis was seen. Immunohistochemistry revealed focal expression of desmin, MyoD1 and myogenin. The previous PPB of this patient was mostly non-viable and fibrotic as the resection was performed after chemotherapy. The viable cells had a primitive aspect, including some rhabdomyoblasts. A few avital chondroid foci were seen. By immunohistochemistry, most cells were positive for desmin, while myogenin was present in only few nuclei and MyoD1 was negative. The previous SLCT showed cystic epithelial lined structures intermingled with a mesenchymal component, consisting of sheets, nests and trabeculae of primitive cells with round to oval nuclei and minimal cytoplasm as well as rhabdomyoblasts. There were multiple mitoses. Necrosis was abundant. The obvious rhabdomyoblastic cells were immunohistochemically positive for desmin, myogenin and MyoD1 in contrast to the more primitive cells.

3.3. Molecular analyses

Results are presented in Table 2. Eight of the ten cases harbored biallelic *DICER1* mutations with a germline mutation in three PPBs and one sarcoma (identified by sequencing of paired blood). For the other cases germline status could not be determined as no normal reference material was available, although the allele frequencies found in cases 1 and 5 were highly suggestive. Case 7 possessed a monoallelic hotspot mutation and case 9 had a variant of unknown significance (VUS), a premature stop in the final exon, omitting a relatively short stretch of 28 amino acids.

Additional mutations in *NRAS*, *KRAS*, *BRAF*, *KMT2C* and *TP53* were detected in six out of the ten neoplasms (cases 1, 2, 4, 5, 9 and 10). Notably, the somatic *DICER1* mutation of the sarcoma of case 10 was the same as in the previous SLCT.

A stable copy number variation (CNV) profile was identified in cases 5 and 7, whereas all the other cases showed several gains and losses with the most common being loss of 17p (including *TP53*) (found in cases 1–4 and 10) and (partial) gain of chromosome 8 (depicted in cases 3–6 and 8–10; Table 3).

RNA expression profiling, successfully carried out on four PPBs and five sarcomas, revealed dissemination within the cluster of ERMSs, which was separate from the other analyzed tumor entities (Fig. 4).

Table 2
Genetic features.

Case	Mutation analysis technique	Somatic *DICER1* mutation (% allele frequency)	Germline *DICER1* mutation (% allele frequency)	Other mutations (% allele frequency)
1	NGS	c.4407_4410delTTCT (p.Ser1470fs); 48.9 % c.5125G > A (p.Asp1709Asn); 48.8 %	Unknown	BRAF (NM_004333.6): c.1799T > A (p.Val600Glu); 46.0 % KMT2C (NM_170606.3): c.5052delA (p.Ala1685fs); 26.35 %
2	WES	c.5425G > A (p.Gly1809Arg); 44 %	c.1783delG (p.Asp595Ilefs*22); 49 %	TP53 (NM_000546.4): c.583A > T (p.Ile195Phe); 59 %
3	WES	c.5125G > A (p.Asp1709Asn); 41.5 %	c.2524delA (p.Met842Cysfs*4); 49 %	None
4 (cerebral metastasis)	WES	c.5425G > A (p. Gly1809Arg); 47 %	c.(2256 + 1_2257-1)_(3269 + 1_3270-1)del (deletion exon 15–20); 51 %	NRAS (NM_002524.4): c.181C > A p.(Gln61Lys); 46 %
5 (cerebral metastasis)	NGS	c.5438A > G (p.Glu1813Gly); 33 % c.2916T > G (p.Tyr972*); 50 %	Unknown	BRAF (NM_004333.6): c.1799T > A (p.V600E); 67 %
6	NGS	c.4206 + 1G > A (p.?); 44 % c.5438A > G (p.Glu1813Gly); 41 %	Unknown	None
7	NGS	c.5439G > T (p.Glu1813Asp); 49 %	Unknown	None
8	NGS	c.5125G > A (p.Asp1709Asn); 27 % c.2468del (p.Gly823fs); 29 %	Unknown	None
9	NGS	c.5683C > T (p.Arg1895*); 48 % VUS	Possible	BRAF (NM_004333.6): c.1799T > A (p.V600E); 91 %
10	WES	c.5438A > G (p.Glu1813Gly); 39 %	c.2257-7A > G, (p.?); 50 %	KRAS (NM_033360.4): c.182A > T p.(Gln61Leu); 38 %

Abbreviations: CNV, copy number variation; NGS, next generation sequencing; p.?, unknown protein effect; WES, whole exome sequencing, x, not performed; VUS, variant of unknown significance.

Table 3
Copy number variations.

Case	Chromosomal gain	Chromosomal loss
1	None	8p; 10p, **17p**
2	1q, 2, 3q, 11q	9p, 10q, **17p**
3	3q, 6q, **8**, 19q	7q, **17p**, 19q
4	1q, 2p, **8**, 15q	10, **17p**
5	**8q**, 11p, 19p, 21q	7q, 11q
6	**8**	14q
7	None	None
8	**8**	None
9	1, 3, 5, 6p, 7p, **8q**, 12, 13, 15, 17q, 18q, 20, 21	6q, 8p
10	2p, **8**, 9p, 12, 13, 14, 17q, 20	10q, **17p**

Gains of chromosome 8 and loss of 17p were most frequent (bold).

Genome-wide DNA methylation profiling was performed on all ten cases; nine cases classified as 'spindle cell sarcoma with RMS-like features, *DICER1*-mutant' [35], all except one (case 3, score 0.8) with an appropriate score $\geq$ 0.9. One PPB (case 4) clustered with ERMSs, also with a score $\geq$ 0.9.

Based upon tSNE analysis, eight cases, including three PPBs (cases 1–3), all four gynaecological sarcoma cases (cases 5–8) and the adolescent case located at the fifth thoracic vertebra (case 10) formed a cluster, whereas the aforementioned PPB (case 4) and the adult sarcoma case of the scapula region (case 6) clustered with ERMS, albeit being relatively closely related to the other *DICER1*-tumors (Fig. 5).

No analysis was feasible on the previous PPB and SLCT of case 10, due to low DNA content.

4. Discussion

DICER1-associated malignancies comprise an enlarging group of related neoplasms. These tumors can arise in a sporadic or hereditary setting, in children and adults, and with a wide anatomic distribution. There are also various developmental disorders based upon *DICER1* mosaicism, bearing a risk for secondary tumorigenesis [36].

In contrast to the broad clinical characteristics, most high-grade/poorly differentiated *DICER1*-associated tumors are histologically similar composed of variable proportions of primitive cells including atypical spindle cells, rhabdomyoblasts, anaplastic cells, blastemal elements and immature or sarcomatous chondroid nodules [1,5,24]. (Neuro)epithelial structures can also be encountered [20,21,26]. The morphology of our PPBs and sarcomas is in concordance with these observations. Nonetheless, as the clinical, histological and immunohistochemical findings are variable, these tumors can be diagnostically challenging. In particular, easily recognizable rhabdomyoblasts may be absent and an aberrant immunophenotype can occur, including diffuse keratin expression (current study, case 6) and positivity for S100, TLE1, SALL4, BCOR or loss of H3K27me3 [23,26,37-44] (see for more details Table 4).

Since poorly differentiated *DICER1*-associated malignancies are polyphenotypic, with varying proportions of mesenchymal, neuroectodermal and epithelial elements, one must assume that *DICER1* mutations affect early precursor cells able to home at various anatomic sites and to differentiate multidirectionally, at least to a certain level [18,39]. This could explain the described overlapping morphological and genetic/epigenetic features that result in variable manifestations of the disease. Yet, low-grade tumors, such as thyroid carcinoma, resemble their corresponding tissue of origin [1].

DICER1 is located on chromosome 14q32.13 and consists of 27 exons. The *DICER1* tumor susceptibility syndrome can be explained by the Knudson's two-hit hypothesis with an inherited germline loss-of-function mutation followed by a post-zygotic somatic missense mutation of the second allele [45]. In sporadic lesions biallelic mutations are also routinely observed. Somatic missense mutations of the *DICER1* gene are almost entirely limited to the RNase IIIb domain in exon 24 and 25, in contrast to germline mutations that are widely distributed throughout the gene and are generally truncating mutations [46]. Indeed, eight of our ten cases harbored biallelic mutations with a confirmed germline origin in three PBBs and one sarcoma; in two other cases germline mutations were suspected. Of note, the somatic *DICER1* mutation (p.Glu1813Gly) in case 10 was the same as detected in the previous SLCT. This specific *DICER1* mutation has been described in SLCT as a low-frequency hotpot mutation (<10 %) and the CNV profiles of both lesions were highly similar. Therefore, a late metastasis should be considered. In one case (case 7) only a monoallelic hotspot mutation was observed and in case 9 a monoallelic variant of unknown significance (VUS) in exon 27, still within the RNAse IIIb domain, was identified. Single missense hotspot mutations were also found in around one third of the *DICER1*-related cerebral RMS-like sarcomas reported by Koelsche et al. [27] and all of these cases, including those of our series, clustered

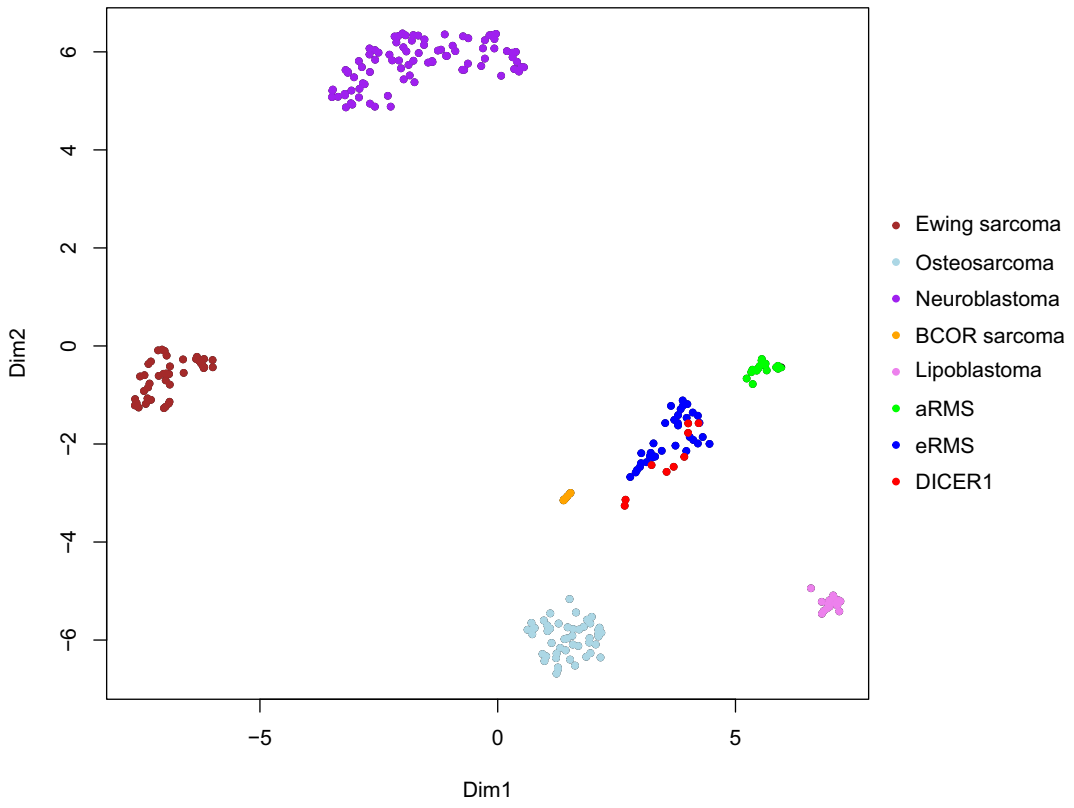

Fig. 4. RNA expression cluster analysis shows a distinct group of our *DICER1* cases within the cluster of ERMS cases.

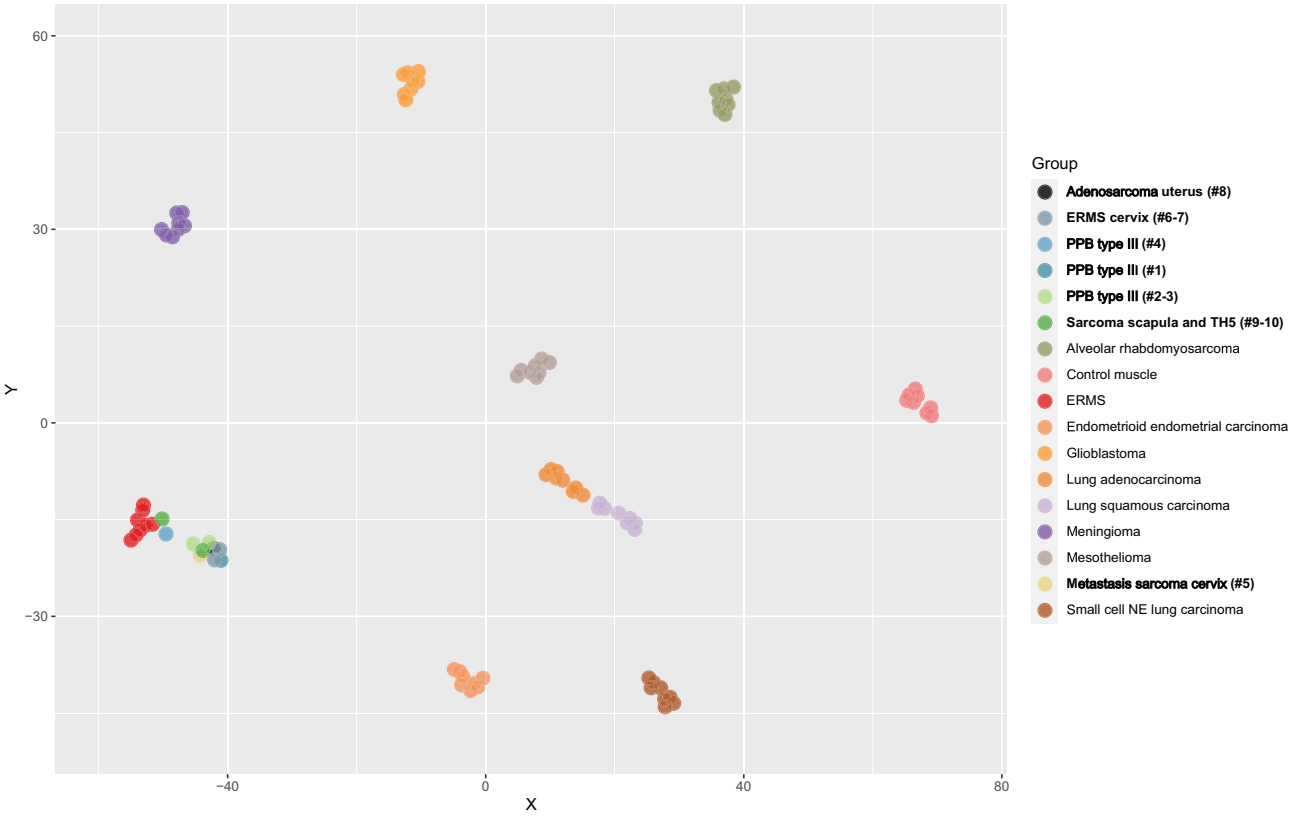

Fig. 5. tSNE cluster analysis reveals comparable methylation profiles of our 10 *DICER1* cases with a close relationship to ERMS.
Abbreviations: ERMS, embryonal rhabdomyosarcoma; NE, neuroendocrine; PPB, pleuropulmonary blastoma; TH5, fifth thoracic vertebra.

Table 4
Immunohistochemical results for *DICER1*-related sarcomas, including PPBs from the literature.

Article	Diagnosis	Positive staining (number of cases)	Negative staining
Gonzalez et al. 2021 [1]	PPB	P53 (62/143 > 25 %)	Not described
Alipour et al. 2021 [41]	PPB	PDL-1 (3/22)	MMR (no loss)
Wu et al. 2016 [10]	Anaplastic sarcoma of kidney (case report)	**Desmin**, p53	**Myogenin**, pancytokeratin, WT1 (N-terminus)
Wu et al. 2018 [8]	Anaplastic sarcoma of kidney (case report)	P53	Not described
Miyama et al. 2021 [42]	RMS of prostate (case report)	**Desmin**, **myogenin**, PAX7, HMGA2, p53	**MyoD1**, MDM2, CDK4, OLIG2, H3K27me3 (no loss)
Yoon et al. 2021 [44]	ERMS of uterine cervix	**Desmin**/**myogenin**/**MyoD1** (1 focal; 1 moderate)	Not described
Bennett et al. 2021 [7]	ERMS of the uterine corpus	**Desmin** (12/12, 10 diffuse and 2 focal), **myogenin** (13/13, 8 focal), **MyoD1** (8/8, 7 focal)	Not described
Kommoss et al. 2021 [28]	ERMS of genitourinary tract	**Desmin** (9/9), **myogenin** (9/9 at least focal)	Not described
Koelsche et al. 2018 [27]	Primary intracranial spindle cell sarcoma with RMS-like features	SMA (17/17), **desmin** (14/17), **myogenin** (5/17, sometimes sparse)	CD34, S100, EMA, CKAE1/3
Sakaguchi et al. 2019 [40]	Primary supratentorial intracranial RMS, *DICER1* mutant	**Desmin**/**myogenin**/ HHF35/myoglobin (2/2, focal); SMA (variable), vimentine (diffuse)	S100, GFAP, EMA, synaptophysin, INI1 (no loss)
Lee et al. 2019 [38]	Intracranial sarcoma	**Desmin** (3/3 focal-patchy), p53 (2/2 overexpression), ATRX (2/2 loss of expression)	**Myogenin** (3/3), SMA, S100, GFAP, OLIG2, cytokeratin
Kamihara et al. 2020 [19]	*DICER1* sarcoma of CNS	**Desmin** (6/6 patchy), **myogenin** (subset of cases, patchy), H3K27me3 (5/5 patchy-complete loss), AFP, p53	Not described
Warren et al. 2020 [23]	*DICER1* sarcomas	**Desmin** (3/3), **myogenin** (3/3), **MyoD1** (2/3; in 1 focal); SALL4 (1/1), p53 (1/1), S100 (1/2), TLE1 (1/1), BCOR (1/1), CD99 (1/1 weak)	CKAE1/3, inhibin A, calretinin, INI1/BRG1 (no loss), GFAP, NKX2.2, SOX10, CD10, CK7, EMA, WT1, CD34, CD68, SMA, synaptofysin, Olig2
Alexandrescu et al. 2021 [43]	Primary intracranial sarcoma, *DICER1* mutant	**Desmin** (4/6), **myogenin** (2/6), H3K27me3 (2/6 minimal/ moderate; 4/6 diffuse), TLE1, CD99 (cytoplasmic-membranous)	SOX2, SOX10, S100, EMA, GFAP, OLIG2, beta-catenin
Roy et al. 2021 [39]	*DICER1*-associated sarcomas	**Desmin** (3/3 patchy-diffuse), **myogenin** (3/3 patchy-diffuse), **MyoD1** (3/3 patchy), CD99 (1/2 patchy)	GFAP, SMA, NSE, synaptofysin, chromogranin, calretinin, INI1 (no loss), S100, SALL4, AFP, CD30, keratin, inhibin, PAX8, WT1, OCT3/4, CD45, TdT Note: a relapse biopsy of one patient was positive for CD99 and SALL4 (diffuse) and synaptofysin and NSE (focal)	Note: a relapse biopsy of one patient was negative for **desmin**, **myogenin** and **MyoD1**
Rossi et al. 2021 [37]	*DICER1*-associated malignancies mimicking germ cell neoplasms	**Desmin** (1/2), **myogenin** (1/2), SALL4 (2/2); H3K27me3 loss (2/2), AFP (1/2), CD56, synaptophysin (1/1 scattered), CD10 (1/1 scattered), CD99 (1/1 weak)	Keratins, CD30, PLAP, S100, Melan-A, EMA, inhibin, calretinin, GFAP, chromogranin, INI1/BRG1 (no loss)
McGluggage et al. 2022 [26]	ERMS/ neuroectodermal tubules in SLCT (1), *DICER1*-associated sarcoma (2), ENT (2)	**Desmin** (3/6), **myogenin** (3/6), **MyoD1** (2/3), SALL4 (4/4 focal-diffuse), CD56 (4/4 diffuse), synaptofysin (5/6 focal-diffuse), chromogranin (2/4 focal), TTF1 (1/1 focal), GFAP (1/5 focal), CD99 (3/5 focal), glypican-3 (1/1 focal), CD117 (1/1 focal), LIN28 (1/2 focal), CD10 (1/1 focal), neurofilament (1/1 focal), vimentin (1/1)	CKAE1/3, MNF116, CAM5.2, EMA, SMA, calretinin, inhibin, PAX8, SF1, WT1, S100, Melan-A, ALK, PLAP, AFP, OCT3/4, CD30, CD45, ER, BRG1 (no loss), INI1 (no loss)

Rhabdomyoblastic markers are depicted in bold.
Abbreviations: CNS, central nervous system; ENT, embryonic-type neuroectodermal tumor; ERMS, embryonal rhabdomyosarcoma; MMR, mismatch repair; PPB, pleuropulmonary blastoma; RMS, rhabdomyosarcoma; SLCT, Sertoli Leydig cell tumor.

within the same methylation group. In addition, RNA-sequencing confirmed affiliation with our other *DICER1* sarcomas (see below).

As *DICER1* alterations in benign and malignant tumors are identical it is hypothesized that the variable malignant potential is due to the presence of additional oncogenic alterations, such as mutations in *RAS* genes and in *TP53* [7,27,28,34,38,47]. The latter is supported by the observation that PPB type 3 shows more diffuse expression of p53 compared to PPB type 1, significantly associated with dismal prognosis [25]. In our cases, mutations in *RAS/RAF* genes were tendentially associated with a worse prognosis. The patient with a PPB bearing an additional *TP53* mutation (case 2) was alive without disease after a short follow-up of 16 months and case 8, without an additional mutation, behaved relatively indolent.

There are various other secondary genetic aberrations described, including mutations, losses and gains/amplifications of e.g. *RET*, *NF1*, *PTEN*, *ATM*, *ATRX*, *WT1*, *FGFR3*, *FGFR4*, *EGFR* and *NTRK3* [23,34,37,47]. Their biological relevance, also in terms of prognosis, remains to be investigated. Interestingly, somatic *DICER1* mutations also occur in sarcomas affecting patients with neurofibromatosis type 1 as reported by Lee et al. [38].

Copy number variations in our cases were miscellaneous with loss of

17p and (partial) gains of chromosome 8 occurring most frequently (Table 3), leading to loss of tumor suppressor genes (such as *TP53* on chromosome 17p) and amplification of oncogenes (such as *MYC* on chromosome 8). This is in line with the results described by Pugh et al. and Roy et al. [39,47].

DICER1 encodes the DICER1 enzyme which is a member of the cytoplasmic endoribonuclease type III family. It processes gene-encoded miRNA precursor hairpins (pre-miRNAs) into mature miRNAs and long double stranded RNA substrates into small interfering RNAs (siRNAs) [46,47]. These small RNAs have key regulatory roles in gene expression [48]. As DICER1 has a central function in organogenesis, all organs are potential targets when this protein is defective. This is also reflected by the different sites of our (sarcoma) cases and all other *DICER1*-manifestations [3,5-7,19-24,27,28]. By RNA expression analysis and genome-wide methylation profiling clustering of our cases was obvious, confirming a strong relationship on genetic and epigenetic level. The distinct epigenetic signature was recently identified for sarcomas of the central nervous system and the genitourinary tract [27,28]. Using both methods a link with ERMS is remarkable which is not surprising when histological and immunohistochemical features are taken into account [1].

Because of the robustness, methylation profiling can be a diagnostic aid for unraveling difficult and exceptional cases.

5. Conclusion

DICER1-associated poorly differentiated neoplasms share morphological, immunohistochemical and (epi)genetic features with some similarities to ERMS. Our results support those of others, that *DICER1*-related high-grade malignancies form a spectrum. As such, it could be debated whether terminology of these neoplasms should be changed to an overarching nomenclature, as suggested by McCluggage et al. [26,49-51].

The broad clinical spectrum with a wide age range and site distribution can be misleading, especially in non-classical cases.

Finally, *DICER1* syndrome is probably more common than previously estimated [52]. Thus, awareness in daily practice helps to counsel and treat patients adequately. Future studies with a larger number of patients will need to be performed in order to consolidate our observations.

Ethical approval

This study was conducted in accordance with the Code of Conduct for Medical Research of the Federation of the Dutch Medical Scientific Societies.

Funding

This research did not receive any specific grant from funding agencies in the public, commercial, or not-for-profit sectors.

Declaration of competing interest

None.

Acknowledgements

We would like to sincerely thank Professor A. von Deimling, Department of Neuropathology, University Hospital Heidelberg, Germany, for his help with interpreting the methylation profiling data and for providing Fig. 5.

References

[1] González IA, Stewart DR, Schultz KAP, Field AP, Hill DA, Dehner LP. DICER1 tumor predisposition syndrome: an evolving story initiated with the pleuropulmonary blastoma. Mod Pathol 2022;35(1):4–22.
[2] Dehner LP, Messinger YH, Schultz KA, Williams GM, Wikenheiser-Brokamp K, Hill DA. Pleuropulmonary blastoma: evolution of an entity as an entry into a familial tumor predisposition syndrome. Pediatr Dev Pathol 2015;18(6):504–11.
[3] Schultz KA, Yang J, Doros L, Williams GM, Harris A, Stewart DR, et al. DICER1-pleuropulmonary blastoma familial tumor predisposition syndrome: a unique constellation of neoplastic conditions. Pathol Case Rev 2014;19(2):90–100.
[4] Pai S, Eng HL, Lee SY, Hsiao CC, Huang WT, Huang SC. Rhabdomyosarcoma arising within congenital cystic adenomatoid malformation. Pediatr Blood Cancer 2005;45(6):841–5.
[5] Dehner LP, Jarzembowski JA, Hill DA. Embryonal rhabdomyosarcoma of the uterine cervix: a report of 14 cases and a discussion of its unusual clinicopathological associations. Mod Pathol 2012;25(4):602–14.
[6] Wu MK, Sabbaghian N, Xu B, Addidou-Kalucki S, Bernard C, Zou D, et al. Biallelic DICER1 mutations occur in Wilms tumours. J Pathol 2013;230(2):154–64.
[7] Bennett JA, Ordulu Z, Young RH, Pinto A, Van de Vijver K, Burandt E, et al. Embryonal rhabdomyosarcoma of the uterine corpus: a clinicopathological and molecular analysis of 21 cases highlighting a frequent association with DICER1 mutations. Mod Pathol 2021;34(9):1750–62.
[8] Wu MK, Vujanic GM, Fahiminiya S, Watanabe N, Thorner PS, O'Sullivan MJ, et al. Anaplastic sarcomas of the kidney are characterized by DICER1 mutations. Mod Pathol 2018;31(1):169–78.
[9] Stewart DR, Best AF, Williams GM, Harney LA, Carr AG, Harris AK, et al. Neoplasm risk among individuals with a pathogenic germline variant in DICER1. J Clin Oncol 2019;37(8):668–76.
[10] Wu MK, Cotter MB, Pears J, McDermott MB, Fabian MR, Foulkes WD, et al. Tumor progression in DICER1-mutated cystic nephroma-witnessing the genesis of anaplastic sarcoma of the kidney. Hum Pathol 2016;53:114–20.
[11] Khan NE, Bauer AJ, Schultz KAP, Doros L, Decastro RM, Ling A, et al. Quantification of thyroid cancer and multinodular goiter risk in the DICER1 syndrome: a family-based cohort study. J Clin Endocrinol Metab 2017;102(5):1614–22.
[12] Vasta LM, Nichols A, Harney LA, Best AF, Carr AG, Harris AK, et al. Nasal chondromesenchymal hamartomas in a cohort with pathogenic germline variation in DICER1. Rhinol Online. 2020;3:15–24.
[13] Schultz KAP, Williams GM, Kamihara J, Stewart DR, Harris AK, Bauer AJ, et al. DICER1 and associated conditions: identification of at-risk individuals and recommended surveillance strategies. Clin Cancer Res 2018;24(10):2251–61.
[14] Yuan Z, Huo X, Jiang D, Yu M, Cao D, Wu H, et al. Clinical characteristics and mutation analyses of ovarian Sertoli-Leydig cell tumors. Oncologist 2020;25(9):e1396–405.
[15] Apellaniz-Ruiz M, McCluggage WG, Foulkes WD. DICER1-associated embryonal rhabdomyosarcoma and adenosarcoma of the gynecologic tract: pathology, molecular genetics, and indications for molecular testing. Genes Chromosomes Cancer 2021;60(3):217–33.
[16] Nadaf J, de Kock L, Chong AS, Korbonits M, Thorner P, Benlimame N, et al. Molecular characterization of DICER1-mutated pituitary blastoma. Acta Neuropathol 2021;141(6):929–44.
[17] de Kock L, Sabbaghian N, Druker H, Weber E, Hamel N, Miller S, et al. Germ-line and somatic DICER1 mutations in pineoblastoma. Acta Neuropathol 2014;128(4):583–95.
[18] Dehner LP, Schultz KA, Hill DA. Pleuropulmonary blastoma: more than a lung neoplasm of childhood. Mo Med 2019;116(3):206–10.
[19] Kamihara J, Paulson V, Breen MA, Laetsch TW, Rakheja D, Shulman DS, et al. DICER1-associated central nervous system sarcoma in children: comprehensive clinicopathologic and genetic analysis of a newly described rare tumor. Mod Pathol 2020;33(10):1910–21.
[20] Nakano Y, Hasegawa D, Stewart DR, Schultz KAP, Harris AK, Hirato J, et al. Presacral malignant teratoid neoplasm in association with pathogenic DICER1 variation. Mod Pathol 2019;32(12):1744–50.
[21] Rooper LM, Bynum JP, Miller KP, Lin MT, Gagan J, Thompson LDR, et al. Recurrent DICER1 hotspot mutations in malignant thyroid gland teratomas: molecular characterization and proposal for a separate classification. Am J Surg Pathol 2020;44(6):826–33.
[22] Chernock RD, Rivera B, Borrelli N, Hill DA, Fahiminiya S, Shah T, et al. Poorly differentiated thyroid carcinoma of childhood and adolescence: a distinct entity characterized by DICER1 mutations. Mod Pathol 2020;33(7):1264–74.
[23] Warren M, Hiemenz MC, Schmidt R, Shows J, Cotter J, Toll S, et al. Expanding the spectrum of dicer1-associated sarcomas. Mod Pathol 2020;33(1):164–74.
[24] Schultz KAP, Nelson A, Harris AK, Finch M, Field A, Jarzembowski JA, et al. Pleuropulmonary blastoma-like peritoneal sarcoma: a newly described malignancy associated with biallelic DICER1 pathogenic variation. Mod Pathol 2020;33(10):1922–9.
[25] González IA, Mallinger P, Watson D, Harris AK, Messinger YH, Schultz KAP, et al. Expression of p53 is significantly associated with recurrence-free survival and overall survival in pleuropulmonary blastoma (PPB): a report from the international pleuropulmonary Blastoma/DICER1 registry. Mod Pathol 2021;34(6):1104–15.
[26] McCluggage WG, Stewart CJR, Belcijan NL, Mourad S, Goudie C, Chan JC, et al. Neuroectodermal elements are part of the morphological spectrum of DICER1-associated neoplasms. Hum Pathol 2022;123:46–58.

[27] Koelsche C, Mynarek M, Schrimpf D, Bertero L, Serrano J, Sahm F, et al. Primary intracranial spindle cell sarcoma with rhabdomyosarcoma-like features share a highly distinct methylation profile and DICER1 mutations. Acta Neuropathol 2018; 136(2):327–37.
[28] Kommoss FKF, Stichel D, Mora J, Esteller M, Jones DTW, Pfister SM, et al. Clinicopathologic and molecular analysis of embryonal rhabdomyosarcoma of the genitourinary tract: evidence for a distinct DICER1-associated subgroup. Mod Pathol 2021;34(8):1558–69.
[29] Steeghs EMP, Kroeze LI, Tops BBJ, van Kempen LC, Ter Elst A, Kastner-van Raaij AWM, et al. Comprehensive routine diagnostic screening to identify predictive mutations, gene amplifications, and microsatellite instability in FFPE tumor material. BMC Cancer 2020;20(1):291.
[30] Wingett SW, Andrews S. FastQ screen: a tool for multi-genome mapping and quality control. F1000Res 2018;7:1338.
[31] 2019 BIPG.
[32] Dobin A, Davis CA, Schlesinger F, Drenkow J, Zaleski C, Jha S, et al. STAR: ultrafast universal RNA-seq aligner. Bioinformatics 2013;29(1):15–21.
[33] Capper D, Jones DTW, Sill M, Hovestadt V, Schrimpf D, Sturm D, et al. DNA methylation-based classification of central nervous system tumours. Nature 2018; 555(7697):469–74.
[34] Koelsche C, Schrimpf D, Stichel D, Sill M, Sahm F, Reuss DE, et al. Sarcoma classification by DNA methylation profiling. Nat Commun 2021;12(1):498.
[35] Koelsche C, Mynarek M, Schrimpf D, Bertero L, Serrano J, Sahm F, et al. Primary intracranial spindle cell sarcoma with rhabdomyosarcoma-like features share a highly distinct methylation profile and DICER1 mutations. Acta Neuropathol 2018; 136(2):327–37.
[36] Venger K, Elbracht M, Carlens J, Deutz P, Zeppernick F, Lassay L, et al. Unusual phenotypes in patients with a pathogenic germline variant in DICER1. Fam Cancer 2021. PMID: 34331184.
[37] Rossi S, Barresi S, Stracuzzi A, Lopez-Nunez O, Chiaravalli S, Ferrari A, et al. DICER1-associated malignancies mimicking germ cell neoplasms: report of two cases and review of the literature. Pathol Res Pract 2021;225:153553.
[38] Lee JC, Villanueva-Meyer JE, Ferris SP, Sloan EA, Hofmann JW, Hattab EM, et al. Primary intracranial sarcomas with DICER1 mutation often contain prominent eosinophilic cytoplasmic globules and can occur in the setting of neurofibromatosis type 1. Acta Neuropathol 2019;137(3):521–5.
[39] Roy P, Das A, Singh A, Panda J, Bhattacharya A, Gehani A, et al. Phenotypic similarities within the morphologic spectrum of DICER1-associated sarcomas and pleuropulmonary blastoma: histopathologic features guide diagnosis in the LMIC setting. Pediatr Blood Cancer 2021;69(3):e29466. Epub.
[40] Sakaguchi M, Nakano Y, Honda-Kitahara M, Kinoshita M, Tanaka S, Oishi M, et al. Two cases of primary supratentorial intracranial rhabdomyosarcoma with DICER1 mutation which may belong to a "spindle cell sarcoma with rhabdomyosarcoma-like feature, DICER1 mutant". Brain Tumor Pathol 2019;36(4):174–82.
[41] Alipour Z, Schultz KAP, Chen L, Harris AK, Gonzalez IA, Pfeifer J, et al. Programmed death ligand 1 expression and related markers in pleuropulmonary blastoma. Pediatr Dev Pathol 2021;24(6):523–30.
[42] Miyama Y, Makise N, Miyakawa J, Kume H, Fukayama M, Ushiku T. An autopsy case of prostatic rhabdomyosarcoma with DICER1 hotspot mutation. Pathol Int 2021;71(1):102–8.
[43] Alexandrescu S, Meredith DM, Lidov HG, Alaggio R, Novello M, Ligon KL, et al. Loss of histone H3 trimethylation on lysine 27 and nuclear expression of transducin-like enhancer 1 in primary intracranial sarcoma, DICER1-mutant. Histopathology 2021;78(2):265–75.
[44] Yoon JY, Apellaniz-Ruiz M, Chong AL, Slim Z, Salfinger SG, Clarke BA, et al. The value of DICER1 mutation analysis in "Subtle" diagnostically challenging embryonal rhabdomyosarcomas of the uterine cervix. Int J Gynecol Pathol 2021;40 (5):435–40.
[45] Thunders M, Delahunt B. Gene of the month: DICER1: ruler and controller. J Clin Pathol 2021;74(2):69–72.
[46] Foulkes WD, Priest JR, Duchaine TF. DICER1: mutations, microRNAs and mechanisms. Nat Rev Cancer 2014;14(10):662–72.
[47] Pugh TJ, Yu W, Yang J, Field AL, Ambrogio L, Carter SL, et al. Exome sequencing of pleuropulmonary blastoma reveals frequent biallelic loss of TP53 and two hits in DICER1 resulting in retention of 5p-derived miRNA hairpin loop sequences. Oncogene 2014;33(45):5295–302.
[48] Song MS, Rossi JJ. Molecular mechanisms of dicer: endonuclease and enzymatic activity. Biochem J 2017;474(10):1603–18.
[49] McCluggage WG, Foulkes WD. DICER1-sarcoma: an emerging entity. Mod Pathol 2021;34(12):2096–7.
[50] McCluggage WG, Foulkes WD. DICER1-associated sarcomas: towards a unified nomenclature. Mod Pathol 2021;34(6):1226–8.
[51] McCluggage WG, Foulkes WD. DICER1-associated sarcomas at different sites exhibit morphological overlap arguing for a unified nomenclature. Virchows Arch 2021;479(2):431–3.
[52] Mirshahi UL, Kim J, Best AF, Chen ZE, Hu Y, Haley JS, et al. A genome-first approach to characterize DICER1 pathogenic variant prevalence, penetrance, and phenotype. JAMA Netw Open 2021;4(2):e210112.